Interaction between Closed-Shell Systems and Metal Surfaces

N. D. Lang
IBM Thomas J. Watson Research Center, Yorktown Heights, New York 10598
(Received 6 November 1980)

The relationship between the van der Waals description of the binding of rare-gas atoms to metal surfaces and the description using a local approximation for exchange-correlation effects is discussed. The local-density treatment is shown to provide a good account of recent data on atomic binding energy, dipole moment, and core-level binding-energy shift. Charge rearrangement maps are used to analyze bond formation and to discuss the validity of the image picture of core-hole screening.

PACS numbers: 68.45.Da, 79.60.Gs, 82.65.Jv, 82.65.Nz

This paper considers the interaction between closed-shell systems, typified by rare-gas atoms, and metal surfaces. These relatively weak interactions are often discussed in terms of the van der Waals mechanism. The hallmark of this mechanism is the power-law dependence of the interaction strength at large metal-adatom separations, which owes its existence to the detachment of the adatom electron from its exchange-correlation hole (image) in the metal. Paradoxically, I demonstrate that a variety of experimental measurements on such systems are well described by a theory—the density functional formalism with local-density approximation for exchange-correlation[1,2]—in which the electron and its exchange-correlation hole are always attached (and which as a result gives an interaction that vanishes exponentially at large distances). Apart from the fact that the local-density theory includes electrostatic and kinetic-energy terms (and hence repulsive forces), it and the van der Waals picture differ simply in the degree of attachment envisioned between an electron and its exchange-correlation hole.[3] The essential point is that for equilibrium rare-gas–metal distances, the most important part of the valence-shell electron orbit (that nearest the metal) lies sufficiently within the surface electron gas that it is most correct to consider the electron to be attached to the hole.

I will discuss experimental data for adsorption on simple metals, and therefore use the jellium model for the metal (ions smeared into a uniform positive background), which is an entirely adequate approximation when treating adatoms that are sufficiently large not to dig into the first layer of metal atoms. The only parameter in this model is the density ρ of the positive background, expressed via r_s ($\frac{4}{3}\pi r_s^3 \equiv \rho^{-1}$). The treatment for a single atom adsorbed on a semi-infinite substrate is fully wave mechanical and self-consistent, and employs the method of Lang and Williams[4] for solving the Hartree-like single-particle equations of the density-functional formalism. These equations contain an effective exchange-correlation potential that is a local potential, and which in the local-density approximation is taken to depend at each point only on the electron density at that point. The only parameter specifying a particular adatom is its nuclear charge Z; the wave functions for the core states are obtained as part of the calculation.

I consider first the ability of the theory to give the measured atomic binding energy. Figure 1 shows this binding energy as a function of metal-adatom distance[5] d, for an Ar atom[6] adsorbed on a substrate of $r_s = 3$ bohrs. [This corresponds to the mean free-electron (s-p) density of Ag, which I will regard as sufficiently like a simple metal in the region of the adatom to use the jellium model for it.] d is measured from the positive-background edge (which by construction is half an interplanar spacing in front of the outermost lattice plane of the crystal being modeled[4]). The

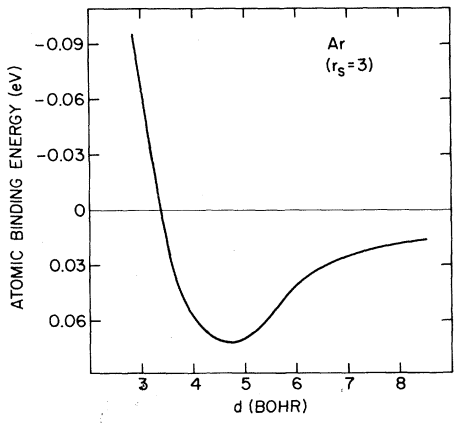

FIG. 1. Atomic binding energy vs distance d for Ar atom on $r_s = 3$ substrate.

atomic binding energy (at equilibrium) is seen to be 0.07 eV; the experiments of Unguris[7] for Ar on Ag(111) at low coverages give 0.074 ± 0.007 eV.

The electron density maps corresponding to different parts of the energy curve exhibit basic aspects of the bonding and, at the shortest distance, the fundamental repulsive interaction responsible for rare-gas scattering. Figure 2 shows density-difference contours (contours of electron density in metal-adatom system, minus superposition of bare-metal and free-atom densities) for three distances. At the largest distance, the contours show a small polarization of the adatom toward the metal; in the equilibrium region, the polarization is more pronounced, and the map shows a resemblance to that for a covalent bond.[4] (Note that it is not appropriate to attribute the binding energy to this polarization; by perturbation theory, the leading term in the binding energy involves only the bare-metal–free-atom superposition.) At the smallest distance, the interaction is strongly repulsive because of Pauli exclusion. The metal charge is pushed out of the way by the closed-shell atom, and piles up in the metal just outside the atom region.

The maps of Fig. 2 show a dipole moment in such a direction as to decrease the substrate work function. I now discuss the common mechanism underlying the formation of this moment in the local-density and in the van der Waals[8] treatments. In the present calculation, the polarization arises from the fact that an electron in the valence shell shows a preference for being on the metal side of the adatom rather than the vacuum side because, on the metal side, the exchange-correlation hole that forms around it is more effective in lowering its energy (the hole is deeper because of the higher electron density on this side).[9] Now recall that as an electron moves from the bulk of a metal out through the surface, the exchange-correlation hole around it lags behind, staying on the surface and becoming the image charge. Furthermore, it is the time-dependent interaction between the valence electron and its image (and the image of the core) that yields the van der Waals interaction. For an atom far outside the surface, and thus in the van der Waals regime, the valence electron shows a preference for the metal side of the adatom because this keeps it closer to its own image (i.e., its exchange-correlation hole). Thus in both cases, the permanent polarization of the atom arises simply from the fact that a valence electron tries to derive the maximum energy benefit from its exchange-correlation hole.

The van der Waals treatment yields an atomic binding energy $\propto (d - d_{\mathrm{vdW}})^{-3}$ and a dipole moment $\propto (d - d_{\mathrm{vdW}'})^{-4}$, with $0 \lesssim d_{\mathrm{vdW}}, d_{\mathrm{vdW}'} \lesssim 1$ bohr.[10] Now these expressions arise, crudely speaking, from averaging the image interaction mentioned above over the valence-electron orbit,[11] which at its nearest point is $\lesssim 1$ bohr from the image plane[12] (the position where the classical image interaction diverges). They thus involve an average of a singular function over a region near the singularity, at least insofar as we insist on using these asymptotic forms at short distances. The local-density approximation lacks the nonlocality included in the image interaction, particularly over the part of the orbit furthest from the metal (where the interaction is small), but it becomes a good approximation over just the part of the or-

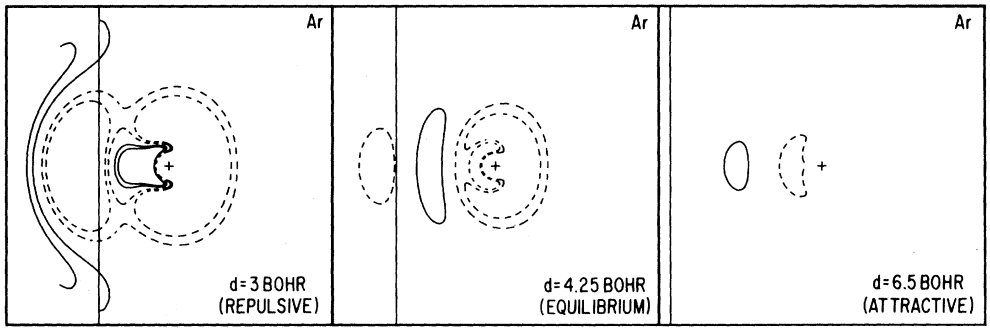

FIG. 2. Density-difference contours for Ar atom ($r_s = 3$ substrate). Maps are plotted in the plane normal to the surface containing the adatom nucleus (+). Metal is to the left; lighter vertical line is positive background edge. Contours are not shown beyond the inscribed circle. Polarization in the core region is deleted because of its complexity. Contour values plotted are $\pm 0.000\,065$ and $\pm 0.000\,13$ electron/bohr^3 (solid line is positive, dashed line is negative).

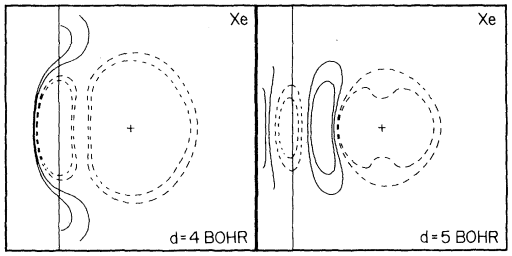

FIG. 3. Density-difference contour maps for Xe on $r_s = 2$ substrate. See caption of Fig. 2 for other details.

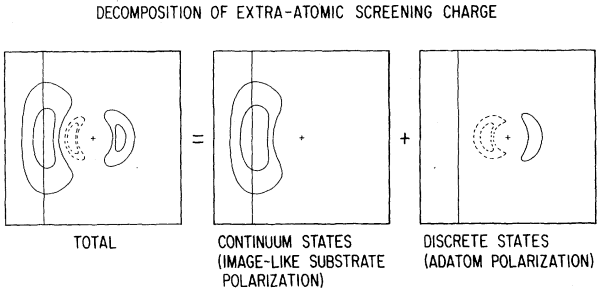

FIG. 4. Contour map of extra-atomic screening charge for Xe ($4d$ core hole; $d = 4.5$ bohrs; $r_s = 4$). Contour values ± 0.0008 and ± 0.0016 electron/bohr^3. See caption of Fig. 2 for other details. Total is decomposed as shown (see text and Ref. 19).

bit for which the effect is largest and the image description least appropriate.

I now compare the values calculated for the dipole moment and the core-level binding-energy shift for Xe with data of Chiang, Kaindl, and Eastman[13] for adsorption on Al(111) ($r_s \approx 2$). An atomic binding-energy curve would be computationally extremely tedious to determine,[14] but I estimate an equilibrium distance $d_{eq} \sim 5$ bohrs, consistent with three independent pieces of information.[15] The first is that the covalent radius of Xe is 0.5 bohr larger than that for Ar (from data on solid rare gases), suggesting from Fig. 1 that $d_{eq} \sim 5$ bohrs for Xe. The second is the low-energy electron-diffraction data of Stoner *et al.*[16] for Xe on Ag(111) (not taken at low coverages however), which gives a distance corresponding to $d_{eq} \approx 4.5$ bohrs. The third is given by Fig. 3, which shows density-difference contours for Xe at $d = 4$ and $d = 5$ bohrs, with the map for $d = 5$ bohrs resembling the Ar map for equilibrium.

The second column of Table I gives a quantity proportional to the dipole moment. The value for $d = 5$ bohrs agrees rather well with the measured value, consistent with the above argument that $d_{eq} \sim 5$ bohrs. The third column gives the difference Δ in core-level binding energy between free atom and adsorbed atom,[17] with good agreement between calculated and measured values. Δ has two components,[17] Δ_c (the chemical or initial-state shift) and Δ_r (the relaxation or final-state shift). Δ_c is not large: at $d = 5$ it is -0.3 eV (and thus $\Delta_r = 1.9$ eV). The simple image model[18] (with static reference plane as in Ref. 12) yields $\Delta_r = 2.0$ eV for this distance, suggesting by the agreement with the calculated value that this model should be adequate for the rare-gas case (in contrast to most other atoms[17]). Note that it is the relatively large separation between core orbitals and image plane that causes the asymptotic form of the image potential to be valid here.

TABLE I. Calculated values: Xe on $r_s = 2$ substrate. Measured values (Ref. 13): Xe on Al(111) substrate. Second column gives rate of change of substrate work function Φ with coverage fraction θ ($\theta = 0$ limit). Dipole moment is $-(d\Phi/d\theta)/4\pi N$, where N is number of atoms per unit area in full layer ($\theta = 1$). Third column gives core-level binding energy shift Δ for $4d$ states.

	$(d\Phi/d\theta)\|_{\theta=0}$ (eV)	Δ (eV)
Calc. $d = 4$	-1.4	1.8
Calc. $d = 5$	-0.6	1.6
Expt.	-0.54 ± 0.04	1.77 ± 0.08

I conclude now by showing that the present calculation can be used to provide a simple understanding of the screening of the core hole that leads to the relaxation shift. A map of extra-atomic screening charge[17] is shown for Xe ($r_s = 4$ substrate[19]) at the left in Fig. 4. This map is not immediately interpretable, but if it is decomposed into discrete and continuum-state contributions,[19] its structure becomes clear. The screening charge is then seen to consist of a rather imagelike distribution, plus an outward polarization of the closed $5p$-$5s$ shell, presumably due simply to a repulsion by the image distribution (and which changes Δ_r by less than 0.1 eV).

I am delighted to acknowledge helpful conversations about this material with A. R. Williams, M. B. Webb, L. W. Bruch, C. D. Gelatt, Jr., M. Scheffler, E. Zaremba, and F. Forstmann.

[1]W. Kohn and L. J. Sham, Phys. Rev. 140, A1133 (1965).

[2]Cf. S. B. Trickey, F. R. Green, Jr., and F. W. Averill, Phys. Rev. B 8, 4822 (1973).

[3]Cf. O. Gunnarsson and R. O. Jones, Phys. Scr. 21, 394 (1980).

[4]N. D. Lang and A. R. Williams, Phys. Rev. B 18, 616 (1978).

[5]Other recent energy calculations (none of which are both wave mechanical and self-consistent) include J. E. Van Himbergen and R. Silbey, Solid State Commun. 23, 623 (1977); L. W. Bruch and Th. W. Ruijgrok, Surf. Sci. 79, 509 (1979); G. G. Kleiman and U. Landman, Solid State Commun. 18, 819 (1976); E. Zaremba and W. Kohn, Phys. Rev. B 15, 1769 (1977); G. Oxinos and A. Modinos, Surf. Sci. 89, 292 (1979).

[6]1*s* shell frozen as described by U. von Barth and C. D. Gelatt, Phys. Rev. B 21, 2222 (1980); all other shells are allowed to polarize.

[7]J. Unguris, Ph.D. thesis, University of Wisconsin, 1980 (unpublished), p. 102.

[8]P. R. Antoniewicz, Phys. Rev. Lett. 32, 1424 (1974). See remarks by R. A. Kromhout and B. Linder, Chem. Phys. Lett. 61, 283 (1979).

[9]The surface electrostatic field also polarizes the atom, but this is a much smaller effect.

[10]E. Zaremba and W. Kohn, Phys. Rev. B 13, 2270 (1976); E. Zaremba, Phys. Lett. 57A, 156 (1976).

[11]P. R. Antoniewicz, Surf. Sci. 52, 703 (1975).

[12]Static image plane at $d = 1.6$ bohrs for $r_s = 2$ [N. D. Lang and W. Kohn, Phys. Rev. B 7, 3541 (1973)]; dynamic image plane somewhat closer to metal (Ref. 10).

[13]T.-C. Chiang, G. Kaindl, and D. E. Eastman (unpublished), and private communication.

[14]The valence state is a sharp resonance in the metal band for the heaviest rare gases on the densest metals, which makes calculations self-consistent enough to extract an accurate energy very tedious.

[15]The first two neglect the difference between Al and Ag for purposes of estimating d_{eq} (note their almost identical lattice constants).

[16]N. Stoner, M. A. Van Hove, S. Y. Tong, and M. B. Webb, Phys. Rev. Lett. 40, 243 (1978).

[17]N. D. Lang and A. R. Williams, Phys. Rev. B 16, 2408 (1977).

[18]G. Kaindl, T.-C. Chiang, D. E. Eastman, and F. J. Himpsel, Phys. Rev. Lett. 45, 1808 (1980); cf. J. W. Gadzuk, J. Vac. Sci. Technol. 12, 289 (1975).

[19]The maps for total screening charge are nearly identical for $r_s = 2$ and $r_s = 4$; but for Xe on $r_s = 2$, the $5p$ states form a resonance, while for $r_s = 4$ they are discrete, and so in the latter case one can conveniently separate the polarization of the closed $5p$ (and $5s$) shells from other screening effects.

Phase Diagrams and Multicritical Points in Randomly Mixed Alloys

David Mukamel [(a)]

IBM Thomas J. Watson Research Center, Yorktown Heights, New York 10598

(Received 14 November 1980)

The Landau-Ginzburg-Wilson model associated with the random alloy $Fe_{1-x}Co_xCl_2$ is analyzed. It is observed that the model includes a coupling term which has thus far been overlooked. Renormalization-group calculations in $d = 4 - \epsilon$ dimensions suggest that the multicritical behavior of this system is *not* associated with the "decoupled" fixed point found in previous theories. This prediction is consistent with recent experiments. A microscopic mechanism which generates this term is considered. It is suggested that similar terms may appear in other quenched alloys.

PACS numbers: 64.60.Kw, 75.10.Jm, 75.50.Ee

Phase diagrams and critical behavior of alloy systems with competing order parameters have been of considerable theoretical[1-5] and experimental[6-10] interest in recent years. Such systems are obtained by mixing two compounds which exhibit two types of magnetic ordering. A simple example is the one in which the two compounds exhibit competing spin anisotropies.[5] Such a system may, in general, be described by an m-component order parameter $\vec{S} \equiv (S_1, \ldots, S_m)$. The first component of the mixture tends to align the first m_1 spin components, $\vec{S}_{\parallel}$, while the other tends to align the remaining (perpendicular) $m_2 (= m - m_1)$ components, $\vec{S}_{\perp}$. Mean-field analysis shows that the phase diagram in the concentration-temperature plane should exhibit two critical lines associated with the transitions from the paramagnetic phase to the two magnetically ordered phases. These lines meet at a multicritical point[11,12] whose nature (whether a bicritical or a tetracritical point) depends on the details of the magnetic interactions in the system. However, recent renormalization-group (RG) studies by Fishman and Aharony[5] (FA) suggest that the phase diagram of

